International Journal of Innovative Technology and Exploring Engineering (IJITEE)
ISSN: 2278-3075 (Online), Volume-8 Issue-12, October 2019

# Feedback Error Learning with Sliding Mode Control for Functional Electrical Stimulation: Elbow Joint Simulation

**Houda Barbouch, Francisco Resquín, Jose Gonzalez-Vargas, Nahla Khraief Hadded, Safya Belghith**

***Abstract: Motivation: Upper-limb motor impairment is one of the most common consequences after Stroke. Limited capability for performing reaching and grasping movements hinders the execution of most activities of daily living. Consequently, the quality lives of the affected individuals are severely compromised. Due to these facts, the recovery of the upper limb functional capabilities is currently one of the keystones of the rehabilitation therapy.***

***Background: Researchers are developing new methods and technologies to boost the outcomes of rehabilitation therapy. A hybrid robotic system has been proposed as a promising rehabilitation technology that combines a passive device (Armeo Spring exoskeleton) to support the arm weight against gravity with a Functional Electrical Stimulation (FES) system to execute the reaching task. This system provides to patients the possibility of training specifically and intensive exercises.***

***Objective: The main objective of this paper is to investigate the performance and robustness of a Feedback Error learning (FEL) scheme mixed with sliding mode control (SMC) to control the FES.***

***Methods: We implemented a nonlinear model describing the muscle response to FES and the dynamic behavior of the elbow joint. Using this model we carried out a simulation study to compare four control strategies: computed torque control (CTC), sliding mode Control (SMC), and adaptive feedback control using FEL: ANN+ CTC and FEL: ANN+SMC. We tested these controllers in two different simulation conditions: In the absence and presence of fatigue. To check the performance of the controllers, we compared the root means square (RMSE) of tracking error and the Normalized RMS of muscle stimulation for various range of movement (ROM).***

***Results: All four controllers achieved good tracking performance in the absence of perturbations. When introducing muscle fatigue, good tracking performance is given essentially by the adaptive control ANN+SMC.***

***Conclusion: Among the proposed approaches, we conclude that the adaptive control (FEL: ANN + SMC) is the most efficient and robust controller, which has been proven by calculating RMSE.***

***Keywords: Sliding Mode Control (SMC), Computed Torque Control (CTC), Feedback Error Learning (FEL), Stroke, Spinal Cord Injury (SCI), Functional Electrical Stimulation (FES).***

## I. INTRODUCTION

Upper-limb motor impairment is one of the most common consequences after Stroke [1]. Limited capability for executing reaching and grasping tasks hinders the execution of most activities of daily living, and consequently decreasing considerably the quality of life of the affected people [2]. After conventional rehabilitation therapy, less than 50 percent of stroke survivors with significant arm paresis recover dexterity in the upper-extremity to carry out functional task [3][4]. For this reason, new rehabilitative methods and technologies have been proposed with the main aim of enhancing the current outcomes, and therefore, increase the quality of life of stroke survivors [5].

Hybrid robotic system has been proposed as a promising rehabilitation technique, providing patients the possibility of training goal-oriented and intensive exercises [6] [7].This system combines a passive device (Armeo Spring exoskeleton) to support the arm weight against gravity with a Functional Electrical Stimulation (FES)system to execute the reaching task.

The use of FES presents several advantages in the rehabilitation field, it improves the motor impairment and reduces the spasticity of the upper limbs [7] [8]. Complementary, it has been also shown that the use of FES could potentially promote cortical plasticity by enhancing the cortical excitability of the descending motor tracts projected to the upper-extremity muscles trained with FES [9] [10]. However, there still are some latent drawbacks that hinder the widely use of FES in clinical settings. These issues arise due to the non-physiological recruitment of motor unit and, the highly non-linear and time-varying response of the musculoskeletal system to FES [6] [11].

**Revised Manuscript Received on October 30, 2019.**
***** Correspondence Author
**Houda Barbouch*,** are with National Engineering School of Tunis, University of Tunis Elmanar, RISC Laboratory, 1002, Tunis, Tunisia.
**Nahla Khraief Hadded,** are with National Engineering School of Tunis, University of Tunis Elmanar, RISC Laboratory, 1002, Tunis, Tunisia.
**Safya Belghith** are with National Engineering School of Tunis, University of Tunis Elmanar, RISC Laboratory, 1002, Tunis, Tunisia.
**Jose Gonzalez-Vargas** is with Cajal Institute, Neural Rehabilitation, Group Consejo Superior de Investigaciones Cientificas, Madrid, Spain.
**Francisco Resquín** is with Catholic University of Asunción. Department of Electronic and Computer Engineering. Paraguay. E-Mails: barbouchhouda@yahoo.fr.

Therefore, the development and implementation of the FES-based controller is one of the current research topics to tackle such limitations. The precise control of the upper-limb joints with FES during reaching is a particular complex problem.

In this regard, different approaches have been presented aimed at boosting the accuracy of the upper-limb response to FES. The main goal is to achieve an accurate response of the musculoskeletal system during the execution of reaching movements. Common approaches consist of feedback strategies [12] [13], feedforward strategies [14] [15] [16] [17], or adaptive controllers that combine the feedback and feedforward strategies [18] [16].

The feedforward strategies have been proposed to use the arm inverse dynamic model in order to approximate the needed motor command and lead the movement execution [14] [15] [16] [17]. However, it is not possible to obtain an accurate direct representation of the inverse dynamics of the arm. Therefore, these approaches use a static approximation. The main limitation of this approach is that it does not account for the actual movement performance. In other words, it cannot compensate for un-modeled dynamics and disturbances.

Alternatively, the feedback approach allows compensating for unexpected disturbances and it provides a stabilized response.

The most widely used feedback controllers are the proportional-derivative (PD) and the proportional-integrative derivative (PID). Despite the great popularity of these strategies, the performance of these controllers is limited because they do not take into account the time-varying and the non-linear response of the musculoskeletal system [19] [20] [21] [22]. More sophisticated feedback controllers, such as sliding mode controllers (SMC) or fuzzy controllers [23] [24], have been proposed. The SMC is a useful and powerful control scheme to deal with the uncertainties, nonlinearities, and bounded external disturbances. However, the main drawback of this controller is chattering problem due to the discontinuous control law acting on the sliding mode when system goes into sliding mode state. On the other hand, adaptive controllers able to adapt to the non-linearity and time-varying behavior of the musculoskeletal system were proposed [25] [26]. These approaches exploits the advantages of both feedforward and feedback controllers with the aim of improving the tracking performance. An interesting approach used the iterative learning control (ILC) algorithm [27], [28]. This strategy modulates the FES intensity (e.g. pulse width) based on the resulting tracking error of previous movements attempts.

The main drawback of this approach is that its performance depends on the accuracy of the arm inverse dynamics model. Furthermore, it is difficult to implement such controller in a real clinical setting since it would require long set up times and the clinician should be knowledgeable on how to set up the many different parameters. Alternatively the feedback error learning (FEL) algorithm implements an artificial neural Network (ANN) to learn the inverse dynamic model of the controller system. In this case, the command output of the feedback controller is used as learning premise to train the ANN during the movement execution. Thus, it simplifies and shortens the adjustment procedure of the controllers because it does not require breaking up the learning and control phases. Other advantages of this approach compared to other adaptive controllers (like the ILC) is that it does not require a known model to operate and only a few parameters are required to setup it up. These features make this strategy an interesting approach for clinical settings. The FEL algorithm has been used to control the wrist [29], [30], ankle and more recently the shoulder and elbow simultaneously in a hybrid configuration (FES + robotics support system), [31]. In these studies, PD and PID feedback controllers were implemented. Taking into account that the learning capability of the ANN depends of the motor command generated by the feedback controller. Therefore we hypothesize that more reliable and robust feedback controllers (such as SMC) could enhance the learning capacity of the ANN, obtaining better performance in upper-limb rehabilitation scenarios.

To test this hypothesis we implemented a simulation framework that allows investigating the performance and robustness various FEL control scheme for upper limb flexion-extension movements of the elbow joint. We carried out a simulation study to compare four control strategies: computed torque control (CTC), and sliding mode Control (SMC), adaptive feedback control using FEL with CTC and SMC strategies.

## II. METHODS

### *A.* Musculoskeletal model

A computational musculoskeletal model of the human upper-extremity was implemented in this study. The musculoskeletal model presented in this section was build considering the following assumption: a) FES is delivered in one muscle at the time, meaning that only one muscle can be active at a time; b) the biceps long head (BLH) muscle and the triceps lateral head (TLH) muscle are considered uniarticular, this mean, the force generated by each muscle generate uniquely torque at the elbow joint; c) the flexion/extension movement of the elbow joint is delimited to the horizontal plane.

The implemented musculoskeletal model involves solely the flexion/extension movement of the elbow joint constrained in the horizontal plane (2D) (see figure 1A). This planar movement constitutes one the most widely scenario for studying and developing FES-based controllers [18], [32]. Additionally, it represents one of the most common scenario in rehabilitation of stroke patients, where the arm is supported against gravity while FES is used for assisting the elbow extension movement [33], [34]. The musculoskeletal model is composed of two antagonistic muscles, the biceps long head (BLH) and the triceps lateral head (TLH), for leading the flexion or extension movement of the elbow respectively (see figure 1A). The range of movement is limited from 0° (elbow fully extended) to 150° (representing maximum flexion of the elbow).

The musculoskeletal model is described considering both the major properties of muscle and segmental dynamics of the arm when led by FES. Therefore, it is composed of two parts: the muscle's model and the equation of motion (arm dynamic), as shown in figure 1B. This mathematical representation allows us to estimate the position (θ), velocity ($\dot{\theta}$) and acceleration ($\ddot{\theta}$) of the elbow joint taking the modulated pulse width (PW) and the frequency of stimulation signal as input.

At the muscle level, a classic hill type representation was used to estimate the generated torque when movement is driven by FES. The same muscle representation presented in literature was implemented [35] [36] [37] such as, it's based on the model proposed by Winters and Stark (1985) [38] and Zhang [37]. The implementation description of this model is fully detailed in Appendix A. In brief, each muscle (BLH and TLH) is represented by its own activation and contraction dynamics as shown in figure 1C. The muscle activation (am) is computed considering the effect of a nonlinear recruitment curve, nonlinear activation frequency relation and a calcium dynamic (first part of figure 1C). Additionally, the effect of muscle fatigue/recovery was included into the model through a fitness function represented by a first-order equation (see Appendix A). This muscle fatigue effect was only considered in the simulation condition 2. Finally, the torque generated by each muscle is calculated from its moment arm and, the combination of the muscle activation, maximum muscle force, the force-length and force-velocity relations (see second part of figure 1C). The simulation study is performed in Matlab/Simulink environment. For the stimulator, the frequency for electrical pulse is fixed on 40Hz and the amplitude is 15mA, then only the pulse width is controlled.

Fig.1 A) Representation of the elbow joint movement considered in this study. B) Block diagram of the musculoskeletal model. C) Muscle model blocks implemented in this study.

### *B.* FES control strategies

The FES controller is aimed at adjusting the delivered current intensity at the target muscles in order to control its response and accurately track a proposed trajectory. The adjustment of the generated torque (at the elbow joint) is performed by modulating the PW of the stimulating signal, while the other FES parameters are kept constant (frequency and signal amplitude).

Considering the highly non-linear response of muscles to FES [6], [11], the compute torque control (CTC) and the sliding mode control (SMC) were implemented in this study. These controllers are two of the most widely non-linear feedback The FES controller is aimed at adjusting the delivered current intensity at the target muscles in order to control its response and accurately track a proposed trajectory. The adjustment of the generated torque (at the elbow joint) is performed by modulating the PW of the stimulating signal, while the other FES parameters are kept constant (frequency and signal amplitude).

Considering the highly non-linear response of muscles to FES [6], [11], the compute torque control (CTC) and the sliding mode control (SMC) were implemented in this study. These controllers are two of the most widely non-linear feedback.

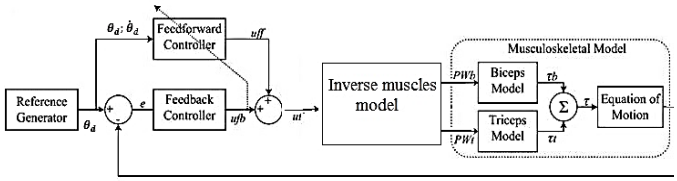


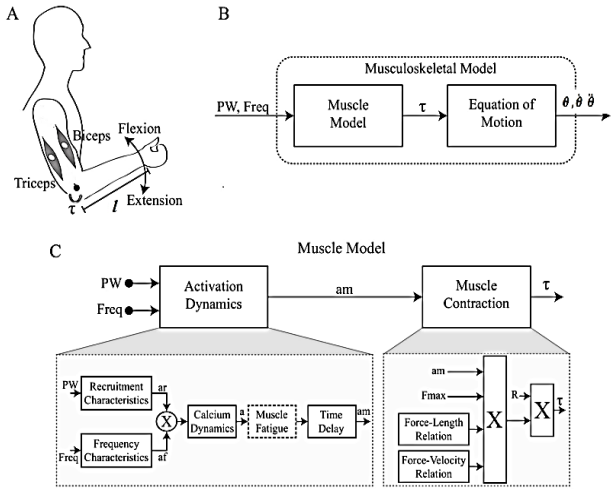


**Fig.2. Functional electrical stimulation (FES) control scheme. Block diagram of the implemented feedback error learning controller for a single joint.**

#### a. FEL algorithm: feedforward + feedback controllers

As shown in figure 2, the feedback error learning (FEL) strategy is formed by the combination of a feedback (CTC or

SMC) and a feedforward (artificial neural network) controller. The FEL is an adaptive controller where the output of the ANN is constantly adjusted to compensate the required elbow torque for achieving accurate tracking motion. The ANN implemented was based on previous studies [29]. It was defined as a three-layer perceptron network, with nine inputs and hidden nodes, and one output node. Both the hidden and output layers have an additional bias node (value -1). The kinematic data of the reference signal is used as input to the ANN. These values were calculated beforehand and they were normalized in the range of -1 to 1 to speed up the learning rates. The weights of the ANN ($w_i$) were initialized with small random values close to zero, and they are updated at each sample time during the movement execution (more detailed in Appendix A).

#### b. Feedback Controllers

**1. Computed torque control**

The CTC is a nonlinear feedback controller that generates the required muscle torque to track the desired trajectory using the control law exposed below:

$$M(\theta)(K_p e + K_v \dot{e} + \ddot{\theta_d} + N(\theta,\dot{\theta})\,\dot{\theta} = \tau_{fb} \quad (1)$$

Where;$(\theta,\dot{\theta},\ddot{\theta})$; are the desired position, velocity, and acceleration respectively; $K_p, K_v$ are the positive diagonal matrices gains and; $M(\theta), N(\theta,\dot{\theta})$ represent the inertia matrix, and the Coriolis matrix of the musculoskeletal system respectively. The gains $K_p, K_v$ was tuned using the polynomial identification method with additional heuristic tuning procedure. The final controller values are shown in the first column of table I. The tuning procedure as well as the comprehensive explanation of the CTC controller is fully detailed in Appendix A.

## 2. Sliding mode control

The sliding mode control is a robust controller for complex high-order nonlinear dynamic plant operating under uncertainty conditions. The SMC consists of forcing the system to tracking trajectories such that, in finite time and in spite of uncertainties, one has a zero position and velocity error respectively ($e + \dot{e} = 0$). The sliding mode control law is described by the following equation:

$$M(\theta)(\ddot{\theta}_d - \lambda\dot{e} - ksign(S)) + N(\theta,\dot{\theta})\,\dot{\theta} = \tau_{fb} \quad (2)$$

where $U_{fb}$ is the control torque ; $S = \lambda e + \dot{e}$ is the sliding surface; $\lambda$,k: are defined as positive diagonal matrices gains; $sat(S/\varphi)$ represents the substitution of the function sign of the convergence law which is the cause of the chattering phenomenon and; the $M(\theta), N(\theta,\dot{\theta})$ represent the inertia matrix, and the Coriolis matrix of the musculoskeletal system respectively. Similar to the tuning procedure of the CTC controller, the controller gains were tuned using the Lyapunov method with additional heuristic tuning procedure. The gain values are shown in the second column of table I. While the detailed explanation of the followed tuning procedure and the controller equation explanations are included in Appendix A.

Table-I: Parameters of the feedback controllers implemented in this study.

| CTC | | SMC | |
|---|---|---|---|
| $K_p$ | $K_v$ | k | λ |
| 120 | 32.86 | 290 | 5.5 |

### c. Reference generation

Motor control studies have demonstrated that natural arm movements, in a free space without obstacle, are quite stereotyped across the population, where the hand paths are straight and the velocity profiles are smooth and bell-shaped [41].

Hogan and Flash derived a mathematical expression to represent the smoothness of arm motion through the solution function that minimizes the third time derivative of position (called jerk) [42]. This mathematical expression is called the minimum jerk trajectory and it relies on a bell-shaped velocity profile. Its use for generating and planning reference trajectory movement results attractive since it only requires one to know the position (initial and target) and desired duration of the movement to completely describe the trajectory with an analytic function of time. The following equation shows the analytical expression used to derive the position reference required at the input of the FEL control algorithm:

$$\theta_r = \theta^s + (\theta^f - \theta^s).\left(10\left(t/d\right)^3 - 15\left(t/d\right)^4 + 6\left(t/d\right)^5\right) \quad (3)$$

Where $\theta^s, \theta^f$ represent the initial and target angles of the i-muscle respectively, $d$ is the movement total duration and $t$ is the current time with $0 \le t \le d$. The velocity and acceleration profiles can be inferred by the first and second-time derivatives. The kinematic profiles defined for an arbitrary target position by the minimum jerk function.

## C. Simulation scenarios

The simulation was performed in the Simulink environment (Mathworks Inc., Natick MA, USA). In the simulation, the frequency and pulse amplitude of the stimulation signal was kept fixed at 40 Hz and 15mA, respectively. While the pulse width of the delivered electrical signal was modulated by the control strategy explained in the previous section. Two different simulation conditions were considered to evaluate the performance of one with controller configuration: SMC alone, CTC alone, SMC+ANN and CTC+ANN.

### a. Scenario 1: absence of muscle fatigue

The first scenario represents the ideal scenario, where a model free-perturbation condition was assumed. In this case, 30 repetitive elbow flexion/extension movements were simulated, where each movement lasted five seconds from the initial to the target positions. Thus, a total runtime simulation of 300 seconds was executed. This condition was used to evaluate the influence of difference range of movement (ROM) on the controller performance, each controller configuration were assessed using four different ROM: (0°-90°); (0°-75°); (0°-60°) and (0°-45°).

### b. Scenario 2: with muscle fatigue

The second scenario was conceived to assess the performance of each controller configuration when the muscle fatigues. Muscle fatigue is one of the most common issues for FES due to the non-physiological recruitment of muscle fibers [6]. In order to simulate the fatigue effect on the muscles, a fitness function was incorporated within the model (see Appendix A). This function was introduced to modify the amount of force produced by each muscle and was modified with two parameters: the muscle fatigue time constant ($T_{fat}$) and the muscle recovery time constant ($T_{rec}$). Two different fatigue conditions were evaluated, corresponding to $T_{fat} = T_{rec} = 95$ seconds and $T_{fat} = T_{rec} = 35$ seconds. 30 repetitive elbow flexion/extension movements considering each ROM were simulated. The fatigue function was activated after 5 movements.

### *D.* Outcome measure

Three metrics were used to compare the controller's performance. The tracking accuracy of each controller to follow the proposed trajectory was evaluated using the root-mean-square error (RMSE) between the reference and simulated joint angle trajectories.

$$\left(RMSE = \sqrt{\frac{1}{n}\sum_{i=1}^{n}(\theta_{ri} - \theta_i)^2}\right) \quad (4)$$

The normalized root-mean-square of the pulse width (PW) delivered at each muscles was calculated to assess the amount of current delivered of each controller configuration. This normalized value was calculated as follow:

$$\mathbf{NRMS_{PW}} = \frac{\sqrt{\frac{(\mathbf{PW})^{\mathbf{T}}(\mathbf{PW})}{\mathbf{n}}}}{\mathbf{max}\,(\mathbf{PW})} \quad (5)$$

In addition, the normalized root-mean-square of the feedback (NRMS$U_{fb}$ ) and feedforward (NRMS$U_{ff}$ ) controllers, were inferred to analyze the contribution of the feedback and feedforward loop given to the total assistance.

$$NRMS_{U_{ff}} = \frac{\sqrt{\frac{(U_{ff})^T(U_{ff})}{n}}}{max\,(U_{ff})} \quad (6)$$

$$NRMS_{U_{fb}} = \frac{\sqrt{\frac{(U_{fb})^T(U_{fb})}{n}}}{max\,(U_{fb})} \quad (7)$$

## III. RESULTS

### A. Scenario1: absence of fatigue (no-disturbance model)

Figure 3 shows the tracking accuracy for one elbow flexion and extension movement driven by controllers' configuration reported in this study (SMC, CTC, SMC+ANN and CTC+ANN) at the range of 0-90º. For this case, the SMC controller reported a RMSE of 2.12º and the CTC 3.44°. When these controllers were combined with the AAN the error were reduced to 1.93° and 3.14° for the SMC +AAN and CTC+AAN respectively. As the muscle fatigue effect was neglected the RMSE value kept constant across the 30 repetitions (runtime of 300 seconds).

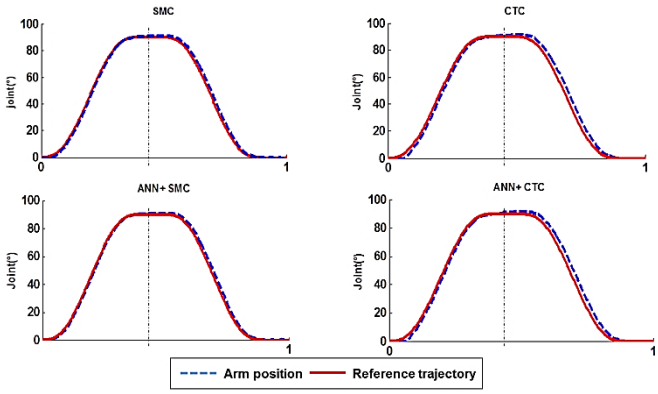


**Fig.3. A representative example of the tracking accuracy when using different controllers' configuration for driving the elbow flexion/extension movement (one cycle). SMC; CTC; ANN+SMC; ANN+CTC .**

Table II shows the RMSE and the NRMSpw score for each controllers' configuration across the different ROM (0°-45°, 0°-60°, 0°-75°, 0°-90°). It is highlighted that the SMC achieved lower RMSE score than the CTC when considering uniquely the feedback controllers for all ROM. While these results were improved (in all cases -ROM-) when the SMC and the CTC were combined with the ANN. Similar results were obtained when assessing the NRMSpw metric for both biceps and triceps muscle. The SMC reported a NRMS score lower than the CTC for all ROM conditions. Again, these values were increased when the SMC and CTC were combined with the ANN (see second part of table II).

### B. Scenario 2: with fatigue

Figure 4 shows the RMSE of each controller configuration across the 30 movements execution when the effect of the muscle fatigue with a ratio of $T_{fat}$=35 and $T_{fat}$=95 was included into musculoskeletal model. The flat responses (in all cases) over the first 5 repetitions correspond to the period of time in which the muscle fatigue was disregarded (fatigue was activated after the fifth movement execution). After |the fifth movement execution, in all cases the RMSE increases as the movement is repeated due to altered response of the muscle model.

The RMSE values for the first, fifteenth and thirtieth movement execution for both simulated fatigue ratio is depicted in table III. When analyzing uniquely the performance of the feedback controllers (SMC and CTC), it can be observed that the SMC achieve smaller error for both fatigue ratio condition. Due to the online learning effects of the ANN these errors were reduced when combined these controller with the ANN, achieving the better performance the SMC+ANN configuration.

**Table-II: The RMSE and the NRMSpw values for each controller configuration across the different ROM (0°-45°, 0°-60°, 0°-75°, 0°-90°)**

| Metric | Controller | Range of movement | | | |
|---|---|---|---|---|---|
| | | 0° – 90° | 0° – 75° | 0° – 60° | 0° – 45° |
| *RMSE*(°) | CTC | 3.4473 | 2.7960 | 2.3835 | 1.7909 |
| | SMC | 2.1215 | 1.8129 | 1.4734 | 1.1157 |
| | ANN+CTC | 3.1433 | 2.5414 | 2.1661 | 1.6267 |
| | ANN+SMC | 1.9319 | 1.7885 | 1.3450 | 1.0328 |
| $NRMS_{pw}$ (Biceps) | CTC | 0.1437 | 0.1343 | 0.0972 | 0.0930 |
| | SMC | 0.1363 | 0.1759 | 0.1102 | 0.1260 |
| | ANN+CTC | 0.1455 | 0.1379 | 0.1000 | 0.0940 |
| | ANN+SMC | 0.1372 | 0.1828 | 0.1216 | 0.1432 |
| $NRMS_{pw}$ (Triceps) | CTC | 0.2241 | 0.2075 | 0.1904 | 0.1571 |
| | SMC | 0.2447 | 0.2903 | 0.2429 | 0.1896 |
| | ANN+CTC | 0.2303 | 0.2131 | 0.1978 | 0.1646 |
| | ANN+SMC | 0.2460 | 0.3233 | 0.2689 | 0.2335 |

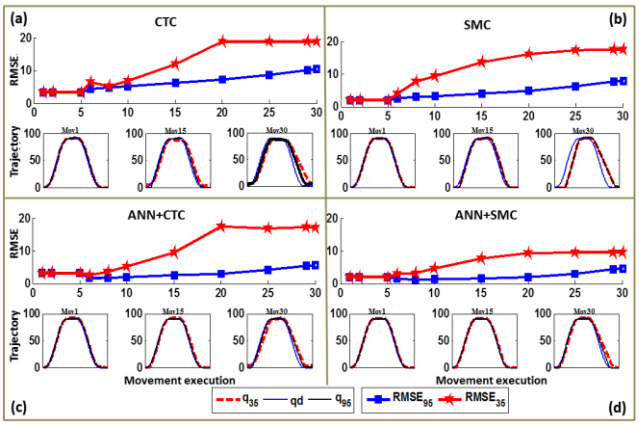


Fig.4. Tracking accuracy of each controllers' configuration over the 30 movements repetition (runtime of 300 seconds) when muscle fatigue function was included. The blue line of the first row represents the RMSE for fatigue factor equals 95s and the red line represents the RMSE for fatigue factor equals 35s The Mov 1 condition represents the first movement (free-perturbation case), Mov 15 is the fifth repletion and the Mov 30 is the last movement execution.

**Table-III: The RMSE values for each controller configuration and simulated ROM over the movement execution number 1, 15 and 30.**

| Simulation condition | Controller | RMSE [°] | | |
|---|---|---|---|---|
| | | Mov 1 | Mov 15 | Mov 30 |
| $T_{fat} = 35s$ | CTC | 3.271 | 11.95 | 18.95 |
| | SMC | 2.015 | 13.57 | 17.45 |
| | ANN+CTC | 3.134 | 9.463 | 16.98 |
| | ANN+SMC | 1.903 | 7.574 | 9.554 |
| $T_{fat} = 95s$ | CTC | 3.271 | 6.207 | 10.43 |
| | SMC | 2.015 | 4.047 | 7.939 |
| | ANN+CTC | 3.134 | 2.465 | 5.664 |
| | ANN+SMC | 1.903 | 1.528 | 4.606 |

THE OVERALL PERFORMANCE ACROSS THE 30 MOVEMENTS' EXECUTION (RUNTIME SIMULATION OF 300 SECONDS) FOR EACH CONTROLLER CONFIGURATION IS SUMMED UP IN FIGURE 5. IT IS DEPICTED THAT REGARDLESS THE VALUE OF THE TFAT PARAMETER (FATIGUE FUNCTION), THE SMC+ANN ACHIEVE THE SMALLEST ERROR OVER THE 30 MOVEMENTS AND THE CTC ALONE THE BIGGEST ERROR. WHEN COMPARED THE PERFORMANCE OF THE FEEDBACK CONTROLLER ALONE, IT CAN BE OBSERVED THAT THE SMC RESULTED IN BETTER PERFORMANCE THAN THE CTC FOR ALL ROM. WHILE, TRACKING ACCURACY IS IMPROVED, IN ALL CASES (ROM AND CONTROLLER CONFIGURATION), WHEN INCLUDING THE ANN. THE OBTAINED RMSE VALUE FOR EACH CONTROLLER AND ROM CONFIGURATION IS DEPICTED IN TABLE IV.

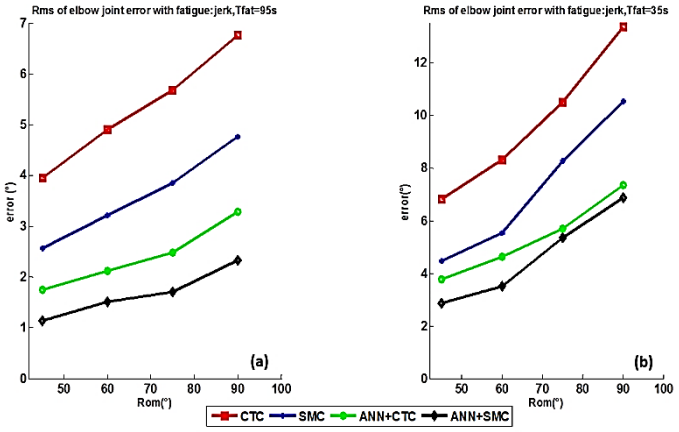


**FIGURE.5. COMPARISON OF THE ROOT MEAN SQUARE OF TRACKING TRAJECTORY (MINIMUM JERK) (A) WITH FATIGUE $T_{FAT}$ =95S, (B) WITH FATIGUE $T_{FAT}$ =35S; FOR CTC, SMC, ANN WITH CTC, AND ANN WITH SMC CONTROLLERS OF THE DIFFERENT RANGE OF MOVEMENT (ROM).**

Figure 6 shows the normalized PW stimulation signal for the four controllers' configuration (SMC, CTC, SMC+ANN, and CTC+ANN) across the movement repetition. The first row represents the $NRMS_{PW}$ for the biceps (red and blue solid lines) and triceps (green and black dashed lines) under the two simulating condition ($T_{fat}$ = 35 and $T_{fat}$ = 90). The smaller rectangles represent the control action of the controller $U$ in black, $U_{ff}$ in red, $U_{fb}$ in bluefor the first, 15th and 30th simulated movement. It can be observed that the NRMSpw increased as the movement is repeated in both muscles and simulation conditions. The achieved NRMSpw score for the first, 15th and 30th simulated movements for each condition is tabulated in table 5. In general terms and in both muscles, the NRMSpw values are increased when combining the feedback controller with the ANN due to the adaptation effect.

**Table-IV: The overall RMSE values for each controller and ROM configuration across the execution of the 30 movements' repetition (runtime of 300 seconds).**

| Simulation condition | Controller | RMSE [°] | | | |
|---|---|---|---|---|---|
| | | 0° – 90° | 0° – 75° | 0° – 60° | 0° – 45° |
| $T_{fat} = 35s$ | CTC | 6.7563 | 5.6784 | 4.9096 | 3.9535 |
| | SMC | 4.7626 | 3.8547 | 3.2182 | 2.5677 |
| | ANN+CTC | 3.2888 | 2.4800 | 2.1275 | 1.7462 |
| | ANN+SMC | 2.3323 | 1.7100 | 1.5150 | 1.1469 |
| $T_{fat} = 95s$ | CTC | 13.3448 | 10.4998 | 8.3157 | 6.8081 |
| | SMC | 10.5173 | 8.2509 | 5.5247 | 4.4727 |
| | ANN+CTC | 7.3504 | 5.6990 | 4.6171 | 3.7627 |
| | ANN+SMC | 6.8574 | 5.3503 | 3.5063 | 2.8576 |

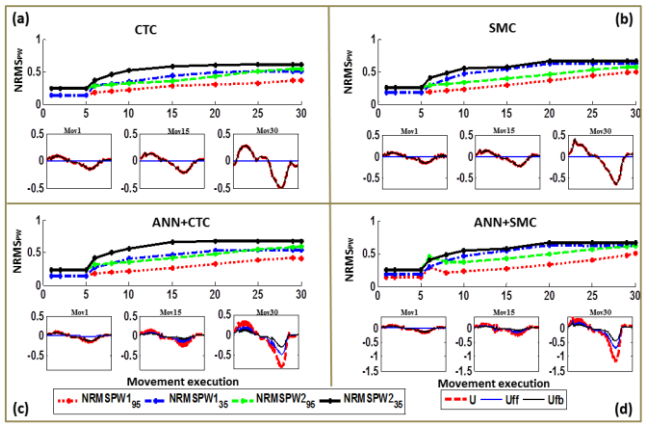


Figure.6. Normalized RMS PW stimulation for the different controllers: (a) The CTC controller, (b) the SMC controller, (c) the ANN + CTC controller and (d) ANN+ SMC controller. For each panel – first row represents the normalized root mean square of PW stimulation $NRMS_{PW}$for the two simulation conditions of both muscles biceps (red colored solid line and blue colored solid line) and triceps (green colored dashed line and black colored dashed line). The second row depicts the output controller ($U, U_{ff}, U_{fb}$) for the first movement (free-perturbation model), the 15th and 30th movement (perturbed model).

**Table-V: The NRMSpw values for each controller configuration across the ROM (0° –90°) in presence of fatigue case.**

| Metric | Simulation condition | Controller | | | |
|---|---|---|---|---|---|
| | | | Mov 1 | Mov 15 | Mov 30 |
| $NRMS_{pw}$ | $T_{fat} = 35s$ | CTC | 0.1379 | 0.4414 | 0.5115 |
| | | SMC | 0.1847 | 0.5464 | 0.6218 |
| | | ANN+CTC | 0.1384 | 0.4666 | 0.5263 |
| | | ANN+SMC | 0.1847 | 0.5464 | 0.6418 |
| | $T_{fat} = 95s$ | CTC | 0.1379 | 0.2824 | 0.3701 |
| | | SMC | 0.1847 | 0.2979 | 0.5741 |
| | | ANN+CTC | 0.2303 | 0.2705 | 0.5050 |
| | | ANN+SMC | 0.1377 | 0.4129 | 0.5945 |

The overall NRMSPW score over the 30 simulated movements for each ROM condition and controller configuration is depicted in figure 7. While the respective values are tabulated in table 6. Panels (a, c) and (b, d) Again, it can be inspected bigger values when considering

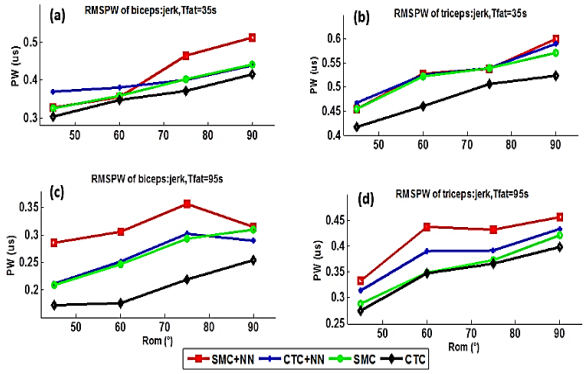


the feedback controllers and the ANN with respect to the values obtained with the feedback controller alone.

Figure.7. Comparison of the root mean square of actuation control(minimum jerk); (a) –(b) with fatigue $T_{fat}$=35s, (c) –(d) with fatigue $T_{fat}$=95s; for CTC, SMC, NN with CTC, and NN with SMC controllers with the same initial angle of 90° and various desired range of movement; (a-c) for biceps and (b-d) for triceps.

## IV. DISCUSSION

We have implemented a simulation framework with the main aim of evaluating the performance and robustness of FES controllers based on the FEL scheme. We consider that this method could potentially benefit the robotic rehabilitation field since it provides a simple, yet powerful adaptive framework. From the results, it is clear that the FEL scheme is able to adapt to fatigue with accuracy and speed. This result is in line with previous results reported in [29], [30], [31], which show the capability of adaptation of the FEL scheme to the highly non-linearity and time-varying response of the musculoskeletal system to the FES.

In this study, the results also point out the superior performance to the FEL scheme compared to purely feedback controllers.

This result is expected since the feedback controller cannot cope with time-varying perturbations such as fatigue.

**Table-VI: The NRMSPW values for each controller**

| Metric | Simulation condition | Controller | movement repetition | | | |
|---|---|---|---|---|---|---|
| | | | 0° – 90° | 0° – 75° | 0° – 60° | 0° – 45° |
| $NRMS_{PW}$ Biceps | $T_{fat} = 35s$ | CTC | 0.3026 | 0.3554 | 0.3709 | 0.4155 |
| | | SMC | 0.3249 | 0.3576 | 0.4032 | 0.4404 |
| | | ANN+CTC | 0.3696 | 0.3554 | 0.4012 | 0.4397 |
| | | ANN+SMC | 0.3273 | 0.3554 | 0.4642 | 0.5122 |
| | $T_{fat} = 95s$ | CTC | 0.1723 | 0.1759 | 0.2186 | 0.2549 |
| | | SMC | 0.2087 | 0.2471 | 0.2937 | 0.3101 |
| | | ANN+CTC | 0.2109 | 0.2521 | 0.3017 | 0.2891 |
| | | ANN+SMC | 0.2863 | 0.3066 | 0.3562 | 0.3115 |
| $NRMS_{PW}$ Triceps | $T_{fat} = 35s$ | CTC | 0.4167 | 0.4598 | 0.5059 | 0.5234 |
| | | SMC | 0.5712 | 0.5220 | 0.4545 | 0.5391 |
| | | ANN+CTC | 0.4678 | 0.5248 | 0.5400 | 0.4900 |
| | | ANN+SMC | 0.4544 | 0.5275 | 0.5375 | 0.6001 |
| | $T_{fat} = 95s$ | CTC | 0.2745 | 0.3468 | 0.3668 | 0.3988 |
| | | SMC | 0.2879 | 0.3491 | 0.3734 | 0.4219 |
| | | ANN+CTC | 0.3136 | 0.3901 | 0.3916 | 0.4340 |
| | | ANN+SMC | 0.3333 | 0.4373 | 0.4317 | 0.4559 |

**configuration across the different ROM** (0° − 45°, 0° − 60°, 0°− 75°, 0° − 90°) in muscle fatigue case.

Similar results have been presented using other adaptive controllers, such as the ILC algorithm [27], [28], [43]. Where it is demonstrated the significant improvements for FES control. However, the mathematical modeling of the musculoskeletal system needed for this approach can become a very complex task. The reason for this difficulty is that it is necessary to realize several assumptions and simplification of the model to capture a reliable description of the system. In this regards, using an ANN can reduce this complexity by learning in real time the inherit mismatches of the model-plant modeling process. Moreover, the ILC requires the adjustment of the controller parameters before being used with each patient. In a real clinical setting, these adjustment procedures can result in a burdensome activity for patients or medical staff. In contrast, when using the FEL controller, a general configuration can be assumed, and the inconsistencies can be compensated automatically through the online learning procedure.

Furthermore, the results show that the tracking results are greatly improved when an SMC is used as the feedback loop. We argue that the reason for this result is that the intrinsic capabilities of the SMC to cope with perturbations allow the ANN to learn a better inverse model of the plant. Once the ANN learns the model, but a disturbance appears (e.g. fatigue), the SMC is able to keep the control stabilized, by its fast dynamic behavior and robustness, while the ANN re-learns the new conditions. Nevertheless, the CTC scheme also yielded good tracking accuracy, but presented higher errors when the motion of range was larger (table 4) and as the movements and fatigue increased (figure 4, table 5). We reason, that this behavior is due to the rigidity of the CTC method to cope with perturbations.

Despite the ANN + SMC scheme yielded better results, the demand on the control output was higher than for the other controllers (figure 6). The SMC is known to present issues due to the chattering of the control output, which could lead to higher energy demands when the system goes into the sliding surface [44], [45]. This point should be further investigated to find the best suitable method to reduce this demand.

Furthermore, this study used a three-layered ANN as a feedforward controller. A latent issue arisen in the use of ANN is its slow convergence of learning [29]. These experimental results show that the network satisfactorily learned within a few iterations. Although no other network topologies were evaluated in this work, the configuration used in this study was chosen based on previous results presented in the literature [31], [30]. Although the analysis of stability and robustness of the controllers was not presented in this works, instability was never observed in all the experiments carried out in this study. Indeed, with the aim of avoiding unexpected response, the parameters of the feedback controller were adjusted to guarantee stability and the ANN was initialized to small random values to compromise the system stability [29], [30].

## V. CONCLUSION

In this simulation study, we hypothesized that a more reliable and robust feedback controller could enhance the learning capabilities of an Artificial Neural Network within a Feedback Error Learning scheme for functional electrical stimulation of the upper arm.

Two configurations of a feedback error learning control strategy were compared against two purely feedback controllers. The comparison was made with a musculoskeletal simulation of the elbow joint taking into account the nonlinearities of muscle contractile properties and the effect of muscle fatigue. We evaluated the performance of four controllers for various conditions.
The results point out that a sliding mode controller does indeed provide a better learning input to the artificial neural network, resulting in better tracking compared to the other approaches. Therefore, this paring learns a more accurate model of the arm and compensate better for fatigue. However, an experimental validation will be done with a hybrid robotic system (Armeo spring + FES).

## APPENDIX A

### A. MODEL EQUATIONS:

#### a) Arm Dynamics

Using Lagrange-Euler method, skeletal dynamics equation is described by:

$$\tau = \left(\frac{1}{4}ml^2 + I\right)\ddot{\theta} + \frac{1}{2}mglcos(\theta) \quad (\boldsymbol{A.1})$$

Where m, l, and I are respectively, the mass, moment of inertia, and length of forearm (Table 1).

#### b) Torque- Force Relationship

As in our study, we have two muscles i.e. two muscle forces. The torque generated by these muscles is obtained as follows.

$$[\tau] = \sigma \begin{bmatrix} F_{a_1} \\ F_{a_2} \end{bmatrix} \qquad (A.2)$$

$$\sigma = [\sigma_B \quad \sigma_T]$$

With $F_{a_i}, \{i = 1,2\}$ the forces developed by biceps and triceps muscle respectively. Coefficients of R the matrix are given in Table 1.

#### c) Muscular forces

In the sequel, each muscle is supposed to be an instantaneous force generator, which means that the muscular force is a nonlinear algebraic function of the muscular activation $a_i, \{i = 1,2\}$.

$$\mathrm{F_{a_i}} = \mathrm{a_i\, f_l(l_i)\, f_v(v_i)\, F_{max_i}} \qquad (A.3)$$

with $l_i$ the length of muscle i, $v_i$ the velocity of muscle i, $F_{max}$ the maximal value of muscular effort. The functions $f_l(.)$ and $f_v(.)$ are the force-length relationship and force-velocity relationship respectively and are described in the following.

#### d) Musculoskeletal geometry

Muscles are linked to bones by tendons. It means that their lengths depend on the articular positions. The relation between muscular fiber length and joint positions reads as:

$$\mathrm{L(\theta) = R.(\theta - \theta_r)} \qquad (A.4)$$
$$\mathrm{V(\dot{\theta}) = R.\dot{\theta}}$$

$\theta_r = \frac{\pi}{2}$: The rest angle, $\theta$: angle position and $L = [l_i]$ (2×1)
$\dot{\theta}$: angle velocity and $V = [v_i]$ (2×1)

#### e) Force-length factor

The relationship between the muscle force and length was described by the model developed by [46] using a Gaussian-like function.

$$f_l(l_i) = exp^{-\left(\frac{\bar{l}_i - 1}{\varepsilon}\right)^2} \qquad (A.5)$$

Where $\mathrm{f_l}$ is a normalized factor that describes the relationship between the muscle force and the muscle length. $\bar{\mathrm{l}}_\mathrm{i}$ is the normalized muscle length.

$$\bar{\mathrm{l}}_\mathrm{i} = \frac{\mathrm{l_i}}{\mathrm{l_{opt_i}}}$$

#### f) Force-velocity factor

The relationship between the muscle force and velocity was described by the model developed by [46]:

$$\mathrm{f_v} = 0.54\tan^{-1}(5.69\mathrm{v} + 0.51) + 0.745 \qquad (A.6)$$

$v = \frac{v_m}{v_{max}}$ : is the normalized muscle velocity;

#### g) Activation dynamics:

This property is the electrical characteristic of muscle; it appears in stimulation of muscle by the electrical pulses.
This muscle part is composed of spatial and temporal summation that acts according to a nonlinear recruitment curve $\boldsymbol{a_{ri}}$, a nonlinear activation-frequency relationship $\boldsymbol{q_f}$, and calcium dynamics $\boldsymbol{a_i}$. [37] [47].
The activation and the relaxation of the muscle cannot be simultaneous For it, there is exists always a time delay. In this case, the Ca² dynamics is defined as follows [48]:

$$\frac{\mathrm{da_i}}{\mathrm{dt}} = \frac{(\mathrm{u_i}^2 - \mathrm{u_i a_i})}{\tau_{ac}} + \frac{(\mathrm{u_i} - \mathrm{a_i})}{\tau_{da}} \qquad (A.7)$$

Where;

$a_i$: represents the muscle activation without fatigue

$$u_i = a_{r_i}.q_f \quad (A.8)$$

$$q_f = \frac{(0.01f)^2}{1 + (0.01f)^2} \qquad (A.9)$$

The injection of an electrical pulse to a muscle activates or recruits a number of muscle fibers. When varying the intensity of the stimulation (i.e. the width or amplitude of the pulses), the number of motor units recruited varies, as does the amount of force generated by the muscle.
The relationship between the level of stimulation and the amount of force produced by the muscle is defined by the recruitment curve (RC). It is generally nonlinear and has a deadband $\boldsymbol{PW_d}$ and saturation $\boldsymbol{PW_s}$.
So, the normalized muscle recruitment curve $\boldsymbol{a_{r_i}}$ was defined as follows:

$$a_{r_i} = \begin{cases} 0 & z_i \le PW_d \\ \dfrac{z_i - PW_d}{PW_s - PW_d} & PW_d < z_i \le PW_s \\ 1 & z_i > PW_s \end{cases} \quad (A.10)$$

Where $z_i$, $i = \{1, 2\}$ is the excitation signal for each muscle.

- **Muscle fatigue:** By stimulating the muscle electrically, the force generated by the muscle will decrease instantaneously. This phenomenon is due to muscle fatigue that depends on the activation level (a) and frequency (f) of the stimulation according to the following equation: [36]

$$\frac{dp}{dt} = \frac{(p_{min} - p)a\lambda f}{T_{fat}} + \frac{(1-p)(1-a\lambda f)}{T_{rec}} \quad (A.11)$$

$$\lambda(f) = 1 - \beta + \beta\left(\frac{f}{100}\right)^2 ; f < 100 \quad (A.12)$$

$$a_{fat}(t) = a(t) * p(t) \quad (A.13)$$

Where;

$p$ : Is the fatigue factor;

$T_{fat}$: The fatigue time constant;

$T_{rec}$: The recovery time constant;

$p_{min}$: The minimum fitness;

$\lambda$: The frequency factor on fatigue;

$\beta$: The shaping factor;

$a_{fat}$: is the activation fatiguing muscle.

### h) Muscle Torque

The torque developed by the muscle is the sum of active torque and passive torque; it is defined as follows:

$$\tau = \tau_a + \tau_p \quad (A.14)$$

$$\tau_a = R * F_{a_i} \quad (A.15)$$

$$\tau_p = -0.2\dot{\theta} - 7.8 \times 10^{-7}\, sign\left(\theta - \frac{\pi}{2}\right) \times \left(e^{-\frac{36}{\pi\left|\theta - \frac{\pi}{2}\right|}} - 1\right) \quad (A.16)$$

The parameter values for the musculoskeletal model of the elbow are listed in table I, which are selected from the literature [46] [47].

**Table VII. Musculoskeletal parameters of the arm model**

| $\tau_{ac}$ [ms] | $\tau_{da}$ [ms] | $PW_d$ [us] | $PW_s$ [us] | $F_{max}$ [N] |
|---|---|---|---|---|
| 40 | 70 | 50 | 400 | 900 |
| $l_{max}$ [m] | $\varepsilon$ | $\sigma$ [m] | $v_{max}$ [m/s] | |
| 0.136(B) 0.084(T) | 0.4 | 0.03(B) -0.03(T) | 0.68(B) 0.42(T) | |

## B. CONTROL STRATEGIES:

### a) Computed Torque Control (CTC):

In this study, we propose to use the nonlinear control law called "Computed Torque Control".

This control strategy allows tracking trajectory of the developed system. Whether, the following control law:

$$\tau_{CTC} = M(\theta)\tau' + N(\theta, \dot{\theta})\dot{\theta} \quad (A.17)$$

By the literature, this control law is based on PD Controller,

So:

$$\tau' = \ddot{\theta}_d + K_p e + K_v \dot{e} \quad (A.18)$$

$$\tau_{ctc} = M(\theta) \times (\ddot{\theta}_d + K_p e + K_v \dot{e}) + N(\theta, \dot{\theta})\dot{\theta} \quad (A.19)$$

$$\begin{cases} e = \theta_d - \theta \\ \dot{e} = \dot{\theta}_d - \dot{\theta} \\ \ddot{e} = \ddot{\theta}_d - \ddot{\theta} \end{cases}$$

Where; $K_p, K_v$ are the matrices gain, they are diagonal and positive definite.

$\theta_d, \dot{\theta}_d, \ddot{\theta}_d$, Are the desired position, velocity, and acceleration respectively.

To insure the stability of the system it is necessary that the following expression of closed loop error dynamics to be verified:

$$\ddot{e} + K_p e + K_v \dot{e} = 0 \quad (A.20)$$

The closed loop characteristic polynomial is:

$$s^2 + K_v s + K_p = 0 \quad (A.21)$$

We assume the standard form for the second order characteristic polynomial as follow:

$$p(s) = s^2 + 2\xi\omega_n s + {\omega_n}^2 \quad (A.22)$$

With $\xi$ the damping ratio and $\omega_n$ the natural frequency. Therefore, desired performance in each component of the error e (t) may be achieved by selecting the PD gains as:

$K_v = 2\xi\omega_n \qquad K_p = {\omega_n}^2$

With $\xi$, $\omega_n$ the desired damping ratio and the natural frequency for joint error. It may be useful to select the desired response at the end of the faster arm, where the masses that must be move are heavier.

It is undesirable for the arm to exhibit overshoot, since this could cause impact if, for instance, a desired trajectory terminates at the surface of a work piece. Therefore, the PD gains are usually selected for critically damping $\xi$=1.5. In this case:

$K_v = 2\sqrt{K_p} \qquad K_p = {K_v}^2/4$

- Selection of the natural frequency: The natural frequency $\omega_n$ governs the speed of response in each error component. It should be large for fast responses and is selected depending on the performance objectives. Thus the desired trajectories should be taken into account in selecting $\omega_n$.

Fig A.1. Synoptic scheme of Computed torque controller (CTC)

**b) Sliding Mode Control (SMC):**

Let the sliding surface of elbow joint is defined as follows:

$$S = \lambda \times e + \dot{e} \qquad (A.23)$$

Where $\lambda$ is a positive factor. Thus, when $S = 0$ is reached, the system checks the tracking error represented by the following equation:

$$\lambda \times e + \dot{e} = 0 \qquad (A.24)$$

Equation $(\boldsymbol{A.20})$ is a first order linear differential equation; it will converge towards zero exponentially.

Having chosen the sliding surface at this stage, the next step would be to choose the control law that will allow error vector $(e, \dot{e})$ to reach the sliding surface. To do so, the control law $\tau_d$ should be designed in such a way that the following condition is met:

$$V = \frac{1}{2} S^2 \qquad (A.25)$$

This function is continuous and strictly positive definite. In order to ensure the stability of the system, the derivative of the Lyapunov function V must be negative. This derivative is expressed as follows:

$$\dot{V} = S \times \dot{S} \; < 0 \quad \forall t \quad (A.26)$$

In order to satisfy this condition, is typically chosen as follows:

$$\dot{S} = -K.\,\mathrm{sign}(S) \; < 0 \quad \forall t \; K > 0 \quad (A.27)$$

We propose,

$$\dot{S} = \lambda \times \dot{e} + \ddot{e} = 0 \qquad (A.28)$$

By $(\mathbf{A.26})$ and $(\mathbf{A.27})$

$$\dot{V} = -S.\,k.\,\mathrm{sign}(S) \qquad \forall t \quad (A.29)$$

The stability of the reaching law is ensured if the gain matrix *k* is diagonal and positive definite. That being said, the equation $(\boldsymbol{A.26})$can be used to reach the sliding surface. By $(\boldsymbol{A.25})$ and$(\boldsymbol{A.26})$, we can conclude the following control law:

$$\tau_{smc} = M(\theta) \times (-\lambda\dot{e} + \ddot{\theta}_d) - k\,\mathrm{sign}(S) + N(\theta, \dot{\theta})\dot{\theta} \quad (A.30)$$

In this paper we have used the method proposed by Slotine [44] and Fallalah [45] to reduce the chattering problem. This method consists on modifying the sign function by a saturation function.

So;

$$\tau_{smc} = M(\theta) \times (-\lambda\dot{e} + \ddot{\theta}_d) - k\,\mathrm{sat}\left(\frac{S}{\varphi}\right) + N(\theta, \dot{\theta})\dot{\theta} \quad (A.31)$$

Where;

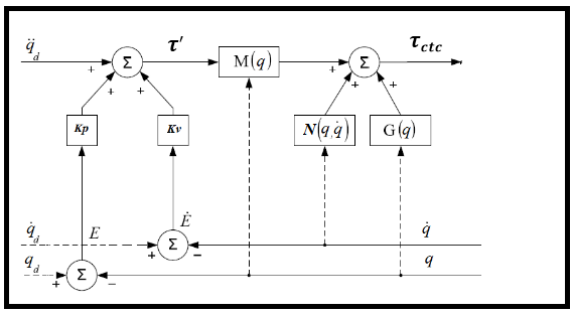


$$sat(S/\varphi) = \begin{cases} 1 & for\ \frac{S}{\varphi} > 1 \\ \frac{S}{\varphi} & for\ -1 < \frac{S}{\varphi} < 1 \\ -1 & for\ \frac{S}{\varphi} < -1 \end{cases}$$

$\boldsymbol{k}$ and $\boldsymbol{\lambda}$ are diagonal positive definite matrices.

Therefore, the control law given in equation $(\boldsymbol{A.31})$ ensures that the control system is stable.

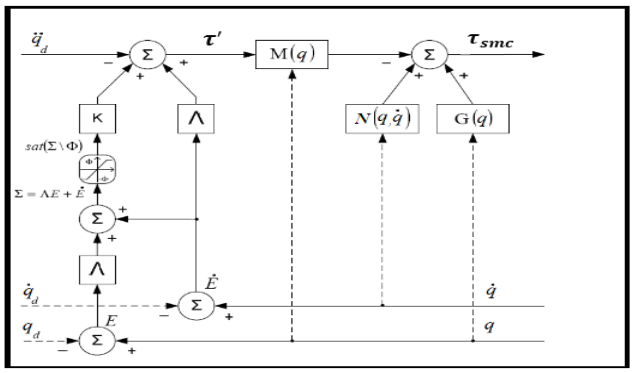


**Fig A.2. Synoptic scheme of Sliding mode control (SMC)**

**c) Feedback Error Learning (FEL):**

The FEL is a scheme that describes the fucntion of the cerebellum for the control of movement. It is an adaptive control, which depends on the feedback Controller ($\tau_{fb}$) to learn a Feed-Forward model ($\tau_{ff}$), . In this study, the feed-forwad model is implemented as a Artificial Neural Network wich is trained at every cycle using the gradient descent algortihm.

$$\bar{\tau}_{ff} = \varphi\left(\ddot{\bar{\theta}}_d, \dot{\bar{\theta}}_d, \bar{\theta}_d, W\right) \qquad (A.32)$$

with

$$\varphi(\ddot{\bar{\theta}}_d, \dot{\bar{\theta}}_d, \bar{\theta}_d, W) = W \times \Phi \qquad (A.33)$$

Where $W$ represents the weights parameter of the ANN; $\Phi = \left[\ddot{\theta}_d\ \dot{\theta}_d\ \theta_d\right]^T$ are the inputs parameters representing the normalized value of acceleration, velocity and joint position. The update procedure is ruled by gradient descend algorithm, described as follow:

$$\Delta\omega_i = -\eta\frac{\partial E}{\partial \omega_i} \qquad \text{for all i} \qquad (A.34)$$

$$E = \frac{1}{2}\bar{\tau}_{fb}^2 \qquad (A.35)$$

$$\frac{\partial E}{\partial W_i} = \frac{\partial E}{\partial \tau_{fb}} \times \frac{\partial \tau_{fb}}{\partial \tau_{ff}} \times \frac{\partial \tau_{ff}}{\partial \omega_i} \qquad (A.36)$$

Where $\Delta\omega_i$ are the weight updating procedure; $\eta$ is the learning rate ranged in the interval from 0 to 1; E represent the error; $\tau_{fb}$ is the output command of the feedback controller and; $\tau_{ff}$is the output action of the ANN in the previous time.

## REFERENCES


1. Peter Langhorne, Julie Bernhardt, and Gert Kwakkel. Stroke rehabilitation. The Lancet, 377(9778):1693–1702, 2011.
2. Gregory P Samsa and David B Matchar. How strong is the relationship between functional status and quality of life among persons with stroke? Journal of rehabilitation research and development, 41(3A):279–82, may 2004.
3. John W Krakauer. Arm function after stroke: from physiology to recovery. In Seminars in neurology, volume 25, pages 384–395, 2005.
4. Peter Langhorne, Fiona Coupar, and Alex Pollock. Motor recovery after stroke: a systematic review. Lancet neurology, 8(8):741–54, aug 2009.
5. M Ferrarin, F Palazzo, R Riener, and J Quintern. Modelbased control of FES induced single joint movements. IEEE Transactions on Neural Systems and Rehabilitation Engineering, 9(3):245–257, 2001.
6. C.L. Lynch and Milos R Popovic. Functional Electrical Stimulation. IEEE Control Systems Magazine, 28(2):40–50, apr 2008.
7. Milos R. Popovic, T. Adam Thrasher, Vera Zivanovic, Jennifer Takaki, and Vlasta Hajek. Neuroprosthesis for retraining reaching and grasping functions in severe hemiplegic patients. Neuromodulation, 8(1):58–72, 2005.
8. T Adam Thrasher, Vera Zivanovic, William McIlroy, and Milos R. Popovic. Rehabilitation of reaching and grasping function in severe hemiplegic patients using functional electrical stimulation therapy. Neurorehabilitation and neural repair, 22:706–714, 2009.
9. Gergely I. Barsi, Dejan B. Popovic, Ina M. Tarkka, Thomas Sinkjær, and Michael J. Grey. Cortical excitability changes following grasping exercise augmented with electrical stimulation. Experimental Brain Research, 191(1):57–66, oct 2008.
10. Teresa J. Kimberley, Scott M. Lewis, Edward J. Auerbach, Lisa L. Dorsey, Jeanne M. Lojovich, and James R. Carey. Electrical stimulation driving functional improvements and cortical changes in subjects with stroke. Experimental Brain Research, 154(4):450–460, feb 2004.
11. Nicola A. Maffiuletti. Physiological and methodological considerations for the use of neuromuscular electrical stimulation. European Journal of Applied Physiology, 110(2):223–234, 2010.
12. James J Abbas and Howard J Chizeck. Feedback Control of Coronal Plane Hip Angle in Paraplegic Subjects using Functional Neuromuscular Stimulation. IEEE Transactions on Biomedical Engineering, 38(7):687–698, 1991.
13. N Lan, P E Crago, and H J Chizeck. Control of end-point forces of a multijoint limb by functional neuromuscular stimulation. IEEE transactions on bio-medical engineering, 38(10):953–965, 1991.
14. Ning Lan, Huan Qing Feng, and Patrick E Crago. Neural Network Generation of Muscle Stimulation Patterns for Control of Arm Movements. IEEE Transactions on Rehabilitation Engineering, 2(4):213–224, 1994.
15. M M Adamczyk and P E Crago. Simulated feedforward neural network coordination of hand grasp and wrist angle in a neuroprosthesis. IEEE Transactions on Rehabilitation Engineering, 8(3):297–304, 2000.
16. G C Chang, J J Luh, G D Liao, J S Lai, C K Cheng, B L Kuo, and T S Kuo. A neuro-control system for the knee joint position control with quadriceps stimulation. IEEE Transactions on Rehabilitation Engineering, 5(1):2– 11, 1997.
17. James J Abbas and Howard Jay Chizeck. Neural Network Control of Functional Neuromuscular Stimulation Systems: Computer Simulation Studies. IEEE Transactions on Biomedical Engineering, 42(11):1117–1127, 1995.
18. Dimitra Blana, Robert F Kirsch, and Edward K Chadwick. Combined feedforward and feedback control of a redundant, nonlinear, dynamic musculoskeletal system. Medical and Biological Engineering and Computing, 47(5 SPEC. ISS.):533–542, 2009.
19. J S Petrofsky, C A Phillips, R Douglas, and P Larson. A computer-controlled walking system: The combination of an orthosis with functional electrical stimulation. Journal of Clinical Engineering, 11(2):121–133, 1986.
20. U Stanic and A Trnkoczy. Closed-loop positioning of hemiplegic patient's joint by means of functional electrical stimulation. IEEE transactions on bio-medical engineering, 21(5):365–70, 1974.
21. Design and simulation of closed-loop electrical stimulation orthoses for restoration of quiet standing in paraplegia. Journal of Biomechanics, 19(10):825–835, jan 1986.
22. J Allin and G F Inbar. FNS control schemes for the upper limb. IEEE transactions on bio-medical engineering, 33(9):818–828, 1986.
23. H Qi, D J Tyler, and D M Durand. Neurofuzzy adaptive controlling of selective stimulation for FES: A case study. IEEE Transactions on Rehabilitation Engineering, 7(2):183–192, 1999.
24. R Davoodi and B J Andrews. Computer simulation of FES standing up in paraplegia: A self-adaptive fuzzy controller with reinforcement learning. IEEE Transactions on Rehabilitation Engineering, 6(2):151–161, 1998.
25. Q Wang, N Sharma, M Johnson, and W E Dixon. Adaptive inverse optimal Neuromuscular Electrical Stimulation. 2010 IEEE International Symposium on Intelligent Control, 43(6):1287–1292, 2010.
26. C Klauer and T Schauer. Adaptive Control of a Neuroprosthesis for Stroke Patients Amplifying Weak Residual Shoulder-Muscle Activity. IFAC-PapersOnLine, 50(1):8792–8797, 2017.
27. Huifang Dou, Kok Kiong Tan, Tong Heng Lee, and Zhaoying Zhou. Iterative learning feedback control of human limbs via functional electrical stimulation. Control Engineering Practice, 7(3):315–325, 1999.
28. D A D.a. Bristow, Marina Tharayil, and A G a.G. Alleyne.A survey of iterative learning control. IEEE Control Systems Magazine, 26(June):96–114, 2006.
29. Kenji Kurosawa, Ryoko Futami, Takashi Watanabe, and Nozomu Hoshimiya. Joint angle control by FES using a feedback error learning controller. IEEE Transactions on Neural Systems and Rehabilitation Engineering, 13(3):359–371, 2005.
30. Takashi Watanabe and Keisuke Fukushima. A Study on Feedback Error Learning Controller for Functional Electrical Stimulation: Generation of Target Trajectories by Minimum Jerk Model. Artificial Organs, 35(3):270–274, 2011.
31. Francisco Resquín, José Gonzalez-Vargas, Jaime Ibáñez, Fernando Brunetti, Iris Dimbwadyo, Laura Carrasco, Susana Alves, Carlos Gonzalez-Alted, Antonio Gomez-Blanco, and José Luis Pons. Adaptive hybrid robotic system for rehabilitation of reaching movement after a brain injury: a usability study. Journal of NeuroEngineering and Rehabilitation, 14(1):104, dec 2017.
32. Kathleen M Jagodnik and Antonie J den Bogert. Optimization and evaluation of a proportional derivative controller for planar arm movement. Journal of biomechanics, 43(6):1086–1091, 2010.
33. Ruth N. Barker, Sandra G. Brauer, and Richard G. Carson. Training of reaching in stroke survivors with severe and chronic upper limb paresis using a novel nonrobotic device: A randomized clinical trial. Stroke, 39(6):1800– 1807, 2008.
34. Chris T. Freeman, A. M. Hughes, Jane H. Burridge, P. H. Chappell, P. L. Lewin, and E. Rogers. Iterative learning control of FES applied to the upper extremity for rehabilitation. Control Engineering Practice, 17(3):368–381, 2009.
35. Robert Riener and Thomas Fuhr. Patient-driven control of FES-supported standing up: a simulation study. Rehabilitation Engineering, IEEE Transactions on, 6(2):113–124, 1998.
36. Sybert Stroeve. Impedance characteristics of a neuromusculoskeletal model of the human arm II. Movement control. Biological Cybernetics, 81(5-6):495–504, 1999.

37. Dingguo Zhang, Tan Hock Guan, Ferdinan Widjaja, and Wei Tech Ang. Functional electrical stimulation in rehabilitation engineering. In Proceedings of the 1st international convention on Rehabilitation engineering & assistive technology in conjunction with 1st Tan Tock Seng Hospital Neurorehabilitation Meeting - i-CREATe '07, page 221, New York, 2007. ACM Press.
38. Jack M Winters and Lawrence Stark. Analysis of Fundamental Human Movement Patterns Through the Use of In- Depth Antagonistic Muscle Models. IEEE Transactions on Biomedical Engineering, BME-32(10):826–839, 1985.
39. a Bartoszewicz and Rj Patton. Sliding mode control.. Journal of Adaptive Control and . . . , XIII:8, 2007.
40. John J Craig. Introduction to Robotics: Mechanics and Control 3rd. Prentice Hall, 1(3):408, 2004.
41. Vincent S Huang and John W Krakauer. Robotic neurorehabilitation: a computational motor learning perspective. Journal of neuroengineering and rehabilitation, 6:5, jan 2009.
42. T Flash and N Hogan. The coordination of arm movements: an experimentally confirmed mathematical model. The Journal of neuroscience : the official journal of the Society for Neuroscience, 5(7):1688–1703, 1985.
43. Hyo-Sung Ahn, YangQuan Chen, Kevin L Moore, Hyo- Sung Ahn, and YangQuan Chen. Iterative Learning Control: Brief Survey and Categorization. IEEE Transactions on Systems, Man, and Cybernetics, Part C: Applications and Reviews, 37(6):1099–1121, 2007.
44. Jean-Jacques Slotine and Weiping Li. Applied Nonlinear Control. 1991.
45. Charles Fallaha. Étude de la Commande par Mode de Glissement sur les système mono et multi variables. 2007.
46. Negin Hesam Shariati, Ali Maleki, and Ali Fallah. Feedforward-feedback P-PID control of elbow joint angle for functional electrical stimulation: A simulation study. Proceedings - 2011 2nd International Conference on Control, Instrumentation and Automation, ICCIA 2011, pages 156–161, 2012.
47. Robert Riener, Maurizio Ferrarin, Esteban Enrique Pavan, and Carlo Albino Frigo. Patient-driven control of FESsupported standing up and sitting down: Experimental results. IEEE Transactions on Rehabilitation Engineering, 8(4):523–529, 2000.
48. P H Veltink and T Sinkjaer. Artificial and natural sensors in FES-assisted human movement control. in Medicine and . . . , (5):0–3, 1998.
49. Houda Barbouch, Jose Gonzalez-Vargas, Jose Luis Pons, Nahla Khraief-Hadded, and Safya Belghith. Sliding mode control for functional electrical stimulation of a musculoskeletal model. 2017 International Conference on Advanced Systems and Electric Technologies (IC_ASET), pages 366–371, 2017


## AUTHORS PROFILE

**Houda Barbouch** received his engineering diploma in "Applied Sciences and Technology- Speciality mechatronics" in 2012 from the High School of Technology and Computer Sciences (ESTI), Tunsia and master's degree in "Automatic and Signal Processing" in 2014 from the National School of Engineering Tunis ENIT, Tunisia. Actually, she is a Ph.D student at the RISC Laboratory in the ENIT, Tunisia. Her research field is focused on Contribution to bio-inspired control algorithm of Functional Electrical Stimultion based rehabilitation therapy for upper limb: Armeo Spring exoskeleton.

**Jose Gonzales-Vargas** obtained a degree in Electronic Engineering Technology Institute of Costa Rica. During this time his studies focused on hardware design, embedded systems and automatic control. In 2006 he was granted the MEXT scholarship from the Japan. This allowed him to obtain his master and doctoral degree in Medical System Engineering in the laboratory of Bio-robotics Assistive Devices from Chiba University. In 2010 he was granted the JSPS young research fellowship, which is the highest ranked scholarship in Japan. After graduating he was a postdoc fellow researcher in the Research Center for Frontier Medical Engineering in Chiba University, as well as a visiting researcher in the Neuro-rehabilitation department of the Medical University of Gottingen. Since July 2013 he has been working as a postdoc researcher in the Neural Rehabilitation group of the Cajal institute in the Spanish National Research Council in Spain.

**NahlaKhraief-Hadded** graduated in Electrical Engineering in 1995 from National School of engineering Sfax. Obtained a master's degree in automatic and industrial automation in 1999 from High School of Science and Technology Tunis, and a PhD in robotics from University of Versailles Saint Quentin in Yvelines France in 2004. Her research interests include the analysis and the control of the nonlinear dynamic systems. She works particularly on the trajectory generation and the control of humanoid robots, the analysis of the chaos and bifurcation of the mechanical systems.

**Safya Belghith** received his engineering diploma in Electrical Engineering (1981) and his D.E.A (1982) and the Ph.D. degree (1985) in Automatic and Signal Processing from the High School of Electricity, Lab Signals and Systems, University Paris XI Orsay. In 1997, she received her Statute Doctorate in Physical Sciences from the Faculty of Sciences Tunis FST with the collaboration of the Laboratory Signals and Systems, at the High School of Electricity University Paris XI Orsay. She is currently a Professor at the National School of Engineering Tunis ENIT, Tunisia and a senior researcher at SysCom Laboratory in the ENIT, Tunisia. His research domain is focused on the analysis of nonlinear systems and chaotic communication, the generation of the pseudo random sequences from chaotic systems and studying their performance in mobile radio communications particularly in a DS/CDMA and on the Synchronization of chaotic systems and its application to secure transmission by chaotic carrier and Cryptography.